Cell Reports

Article

Persistent fatty acid catabolism during plant oil synthesis

Graphical abstract

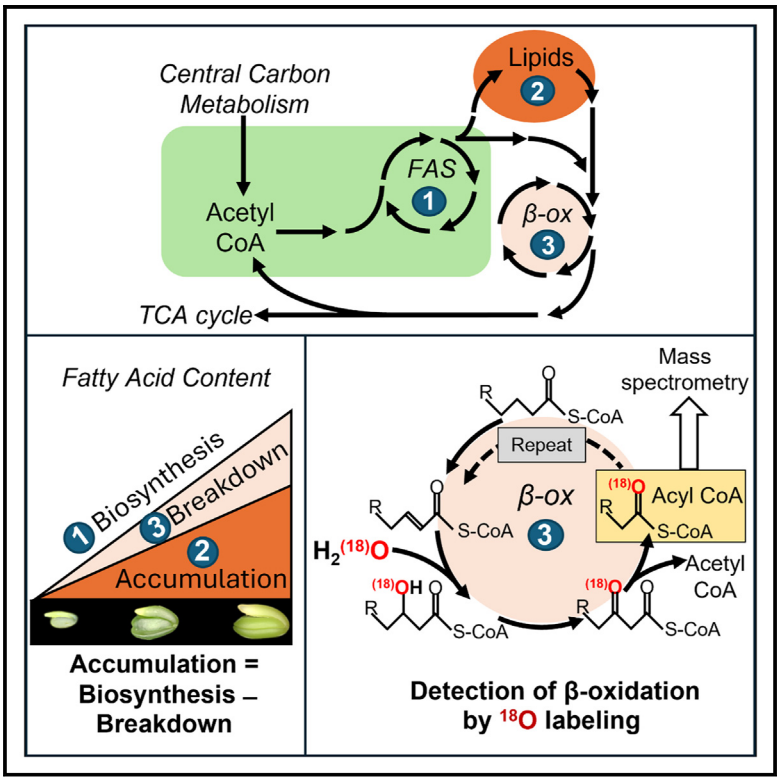

Highlights

- ^{18}O-water incorporation into specific acyl-CoAs unambiguously indicates β-oxidation
- Fatty acid synthesis and oxidation occur concurrently during oilseed development
- Substantial oxidation, comparable to germinating seedlings, initiates early in seed filling
- β-oxidation occurs during the day and night and is a regular aspect of cellular metabolism

Authors

Somnath Koley, Poonam Jyoti, Maneesh Lingwan, ..., Jay J. Thelen, Dong Xu, Doug K. Allen

Correspondence

skoley@danforthcenter.org (S.K.), doug.allen@ars.usda.gov (D.K.A.)

In brief

Koley et al. indicate that fatty acid oxidation occurs concomitantly with fatty acid biosynthesis in multiple plant tissues, including seeds that are thought to stably house storage reserves. This study suggests that some lipid breakdown and fatty acid oxidation is the rule and not the exception in plant metabolism.

Koley et al., 2025, Cell Reports *44*, 115492
April 22, 2025 Published by Elsevier Inc.
https://doi.org/10.1016/j.celrep.2025.115492

Cell Reports

CellPress
OPEN ACCESS

Article

Persistent fatty acid catabolism during plant oil synthesis

Somnath Koley,[1,6,*] Poonam Jyoti,[1] Maneesh Lingwan,[1] Michael Wei,[1] Chunhui Xu,[2,3] Kevin L. Chu,[1] Russell B. Williams,[1] Abraham J. Koo,[4] Jay J. Thelen,[3,4] Dong Xu,[2,3] and Doug K. Allen[1,5,7,*]

[1]Donald Danforth Plant Science Center, St. Louis, MO 63132, USA
[2]Department of Electrical Engineering and Computer Science, University of Missouri, Columbia, MO 65211, USA
[3]Christopher S. Bond Life Sciences Center, University of Missouri, Columbia, MO 65211, USA
[4]Department of Biochemistry, University of Missouri, Columbia, MO 65211, USA
[5]US Department of Agriculture-Agricultural Research Service, St. Louis, MO 63132, USA
[6]X (formerly Twitter): @Koley_Som
[7]Lead contact
*Correspondence: skoley@danforthcenter.org (S.K.), doug.allen@ars.usda.gov (D.K.A.)
https://doi.org/10.1016/j.celrep.2025.115492

SUMMARY

Plant lipids are an essential energy source for diets and are a sustainable alternative to petroleum-based fuels and feedstocks. Fatty acid breakdown during seed germination is crucial for seedling establishment but unexpected during seed filling. Here, we demonstrate that the simultaneous biosynthesis and degradation of fatty acids begins early and continues across all phases of oil filling and throughout the photoperiod. Tests in camelina, rapeseed, and an engineered high-oil tobacco line confirmed that concomitant synthesis and breakdown in oil-producing tissues over development is the rule rather than the exception. Furthermore, we show that transgenics, designed to elevate fatty acid biosynthesis, failed to achieve anticipated increases in storage lipid levels due to increased degradation, potentially explaining the underperformance of engineered lines compared to expectations more generally.

INTRODUCTION

Lipids are a highly desirable renewable feedstock for fuels and polymers as part of a sustainable bioeconomy because they are energetically dense, containing twice the energy of carbohydrates per gram.[1–3] The demand for lipids is expected to double by 2050; however, renewable sources of oil, including oilseeds, are currently insufficient to fulfill societal needs. Efforts to increase oil levels in seeds have focused on enhancing fatty acid[4] and lipid biosynthesis,[5–7] or altering the supply of carbon precursors,[8] approaches that implicitly assume that lipid levels are regulated by inputs. However, lipid gains have been modest, suggesting that other processes contribute to final oil concentrations. One possibility is that potential engineered increases in lipid production are offset by enhanced fatty acid breakdown, resulting in billions of dollars in lost potential productivity worldwide[9] (Methods S1). To assess this possibility, we focused on developing sensitive methods to distinguish synthesis and turnover processes.

Lipid breakdown has been studied extensively at particular stages of the plant life cycle. Germination involves the breakdown of lipid-derived fatty acids in the peroxisome to generate carbon skeletons and energy that sustain the growth of seedlings. Apart from germination, significant oxidation of fatty acids is thought to be limited to maturation of seeds and leaves, including those that have been genetically altered,[10–14] although the process may be active at other times in plant tissues to detoxify cells.[15–17] Lipid remodeling to adjust membrane composition, signaling, and jasmonic acid synthesis have been extensively studied during stress conditions.[18–20] Despite this extensive literature, the quantitative breakdown of fatty acids as a part of normal growth[21] has received far less attention, particularly at developmental stages when significant oil is accumulated. This may in part be due to the challenge of assessing concomitant biosynthesis and breakdown fluxes, which requires the use of isotopes.[22,23]

Active fatty acid breakdown produces short-chain acyl-coenzyme As (CoAs), with 4–14 carbons. Because these are, with a few exceptions,[24] never intermediates in biosynthesis, they serve as an unambiguous signature of fatty acid degradation and recycling. While biosynthesis of fatty acids adds 2-carbon acetyl groups to an acyl-carrier protein (ACP) backbone in the chloroplast,[25,26] breakdown cleaves 2-carbon units from an acyl chain attached to CoA, a process known as β-oxidation[21] (Figure 1A). The process was first observed in dogs[27] and detailed later in plant glyoxysomes (or peroxisomes) in association with glyoxylate activity in seedlings.[28] The breakdown is initiated by acyl-CoA oxidase (ACX1–4) activities specific to chain lengths,[15,29–32] with specific enzymes involved in handling double bonds originating from polyunsaturated fatty acids.[20,21,33,34] Intermediates in the process, including enoyl and ketoacyl-CoAs, form in both chain elongation and breakdown; however,

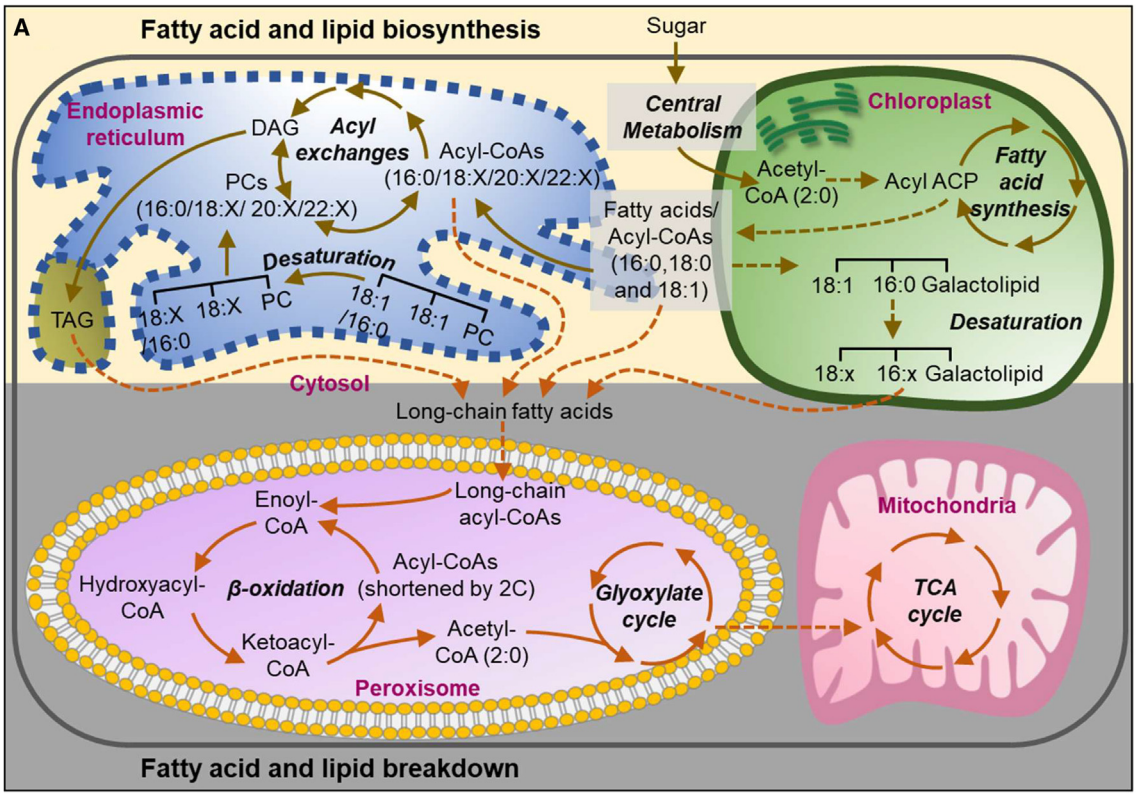

B Fatty acids	Signature CoAs exclusive to fatty acid breakdown
16:0/18:0/20:0/22:0/24:0	*Acyl*-**14:0, 12:0**, 10:0, 8:0, 6:0, 4:0; *Enoyl*-**14:0**, 12:0, 10:0, 8:0, 6:0, 4:0; *Ketoacyl*-**14:0**, 12:0, 10:0, 8:0, 6:0, 4:0
16:1/18:1/20:1/22:1/24:1	*Acyl*-**16:1, 14:1**, 10:0, 8:0, 6:0, 4:0; *Enoyl*-**14:1**, 12:0, 10:0, 8:0, 6:0, 4:0; *Ketoacyl*-**14:1**, 12:0, 10:0, 8:0, 6:0, 4:0
16:2/18:2/20:2/22:2/24:2	*Acyl*-**16:2, 14:2, 10:1**, 8:0, 6:0, 4:0; *Enoyl*-**16:2, 14:2, 12:1**, 10:0, 8:0, 6:0, 4:0 *Dienoyl*-**10:0**; *Ketoacyl*-**16:2, 14:2, 12:1**, 10:0, 8:0, 6:0, 4:0
16:3/18:3	*Acyl*-**16:3, 14:3, 10:2, 8:1**, 4:0; *Enoyl*-**18:3, 16:3, 14:3, 12:2, 10:1, 8:1**, 6:0, 4:0 *Dienoyl*-**10:1**; *Ketoacyl*-**16:3, 14:3, 12:2, 10:1, 8:1**, 6:0, 4:0

Figure 1. Fatty acid and lipid metabolism in plants

(A) Fatty acid and lipid biosynthesis occur in the chloroplast and endoplasmic reticulum (ER), respectively. Generation of polyunsaturated fatty acids takes place on a lipid backbone. Fatty acid breakdown occurs in the peroxisomes of plants. Acetyl-CoA, which is produced during fatty acid oxidation, is converted into organic acids via the glyoxylate cycle before being transported to the mitochondria for further metabolism.

(B) Short- to medium-chain CoAs are characteristic of breakdown of different fatty acids. Breakdown-specific CoAs in orange are specific to fatty acid substrates. TCA, tricarboxylic acid; X, polyunsaturation (see also Data S1).

intermediates with shorter than 20 carbons in acyl chain are exclusively involved in β-oxidation. Furthermore, unsaturated shorter-chain CoAs are specifically derived from polyunsaturated fatty acids (Figure 1B) and unequivocally indicate lipid degradation because the process of adding multiple double bonds to form polyunsaturated fatty acids in plants occurs exclusively on a lipid backbone[12,35,36] (Figure 1A). Saturated acyl-CoAs associated with β-oxidation in germinating seedlings were measured,[30,31,37] but the levels of oxidation in other plant tissues, including developing seeds that are concentrated in oil and provide the economic value of crops, remain unclear. Here, we present multiple lines of evidence that fatty acid oxidation occurs concomitantly with oil synthesis in oil-rich tissues throughout development. The processes are finely controlled throughout the photoperiod and were pronounced in lines engineered for increased oil.

RESULTS AND DISCUSSION

We developed a mass spectrometry (MS) method to sensitively measure acyl-CoAs, extending descriptions in the literature[37] (Methods S2) to analyze intermediates in the oxidation cycle originating from the breakdown of saturated and unsaturated fatty acids (Figure 1B). The method was initially evaluated in

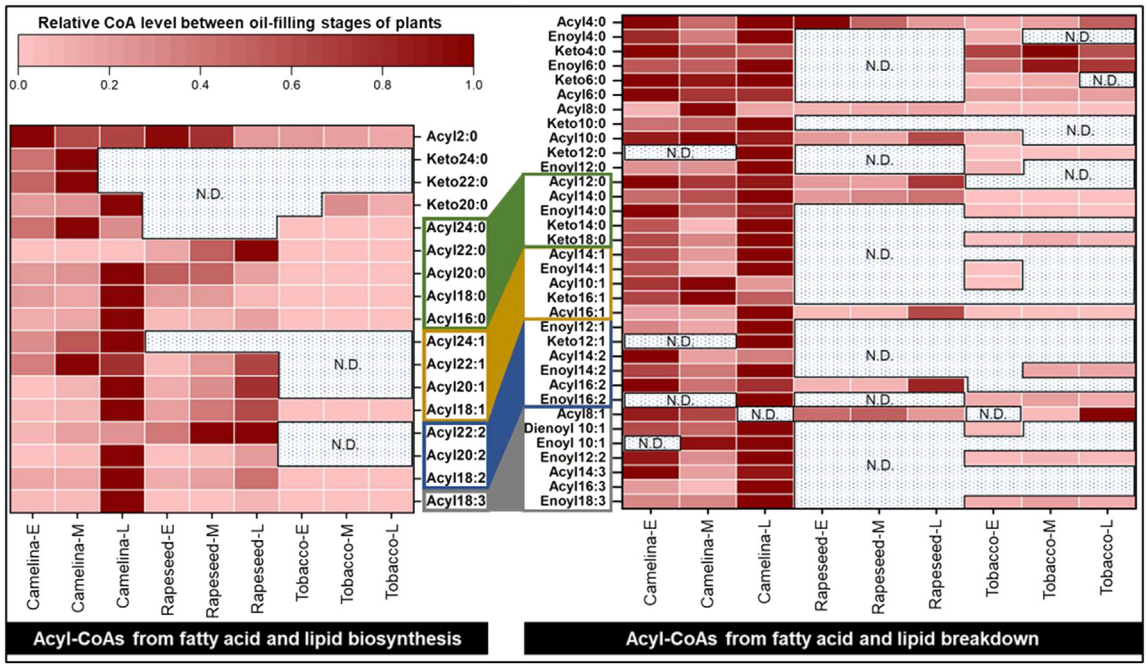

Figure 2. Dynamic fatty acid and lipid metabolism at stages of oil filling

Relative level of fatty acid biosynthesis (left) and breakdown-specific (right) CoAs from camelina (*Camelina sativa*) and rapeseed (*Brassica napus*) seeds and high-oil tobacco (*Nicotiana tabacum*) leaves in early (E), middle (M), and late (L) development. CoAs representative of a specific unsaturated group of fatty acids are grouped together with same color border. CoAs that overlap in synthesis and breakdown are listed in the synthesis steps. N.D., not detected. Heatmaps show mean value ($n = 3$). t tests are presented in Data S2. A value of one on the scale bar indicates the largest peak area of a specific CoA across nine conditions, with smaller numbers presented as relative values.

camelina seedlings, where fatty acid breakdown is expected and is an essential process of germination. We discovered shorter-chain unsaturated acyl-CoAs, which have not been previously measured in plants, indicating conclusively that breakdown included acyl chains with a lipid origin. Saturated and unsaturated forms of acyl-, enoyl-, dienoyl-, and ketoacyl-CoAs were detected that are signatures of fatty acid oxidation (Figure S1; Methods S2).

Fatty acid biosynthesis and breakdown is a synchronized process

As seeds in many plants have high concentrations of lipids, even a small amount of fatty acid recycling during seed filling could dramatically affect the final composition. To assess whether breakdown occurs even at times of significant fatty acid biosynthesis, three developmental stages were measured in camelina (15, 20, and 25 day post-anthesis [DPA]) and rapeseed (15, 25, and 35 DPA) during seed development. In addition, CoA levels were measured in the leaves of transgenic high-oil tobacco[38] (30, 45, and 60 days after sowing). The stages were defined to capture oil biosynthesis after initiation (the first stage, early), at the highest rate of oil biosynthesis (the second stage, mid), and at the final phase of filling (the third stage, late), when tissues were still green and prior to desiccation or senescence (Figure S2). A total of 51 esterified CoAs were quantified, including saturated and unsaturated forms of acyl-, enoyl-, and ketoacyl-CoAs, 34 of which were specific to breakdown processes (Figure 2).

The presence of unsaturated short- to medium-chain CoAs in all samples indicated that oxidation included the breakdown of lipids specifically during oil filling. Both synthesis- and breakdown-specific CoAs reached their highest levels at later stages of seed development, indicating that lipid biosynthesis and breakdown are finely controlled when seed lipid levels approach maximum values. β-Oxidation-specific CoAs were abundant in camelina seeds and engineered tobacco leaves, but more limited in rapeseed. Consistent with our result, prior work including enzymatic assays and ^{14}C feeding experiments in engineered rapeseed lines described measurable β-oxidation activity.[17] Rapeseed produces less linoleic acid (18:2) and linolenic acid (18:3) and more erucic acid (22:1) (Figure S3), which may reflect a reduced turnover of very-long-chain fatty acids. In essence, the presence of fewer long-chain acyl-CoAs for acyl editing in endoplasmic reticulum to make polyunsaturates (e.g., 18:2, 18:3) in rapeseed could also result in a reduced availability for β-oxidation. Furthermore, a recent ^{14}C study in engineered high-oil tobacco[39] indicated that lipid degradation occurs in tissues actively accumulating lipids; however, the reactions of β-oxidation were not extensively investigated. When we examined concurrent synthesis and breakdown of fatty acids in transgenic high-oil tobacco leaves (Figure 2), the results indicated that triacylglycerol (TAG) production was partially unstable and was likely being degraded through β-oxidation.[39,40] Thus, engineering efforts must consider the collateral effects of breakdown from enhanced lipid production.

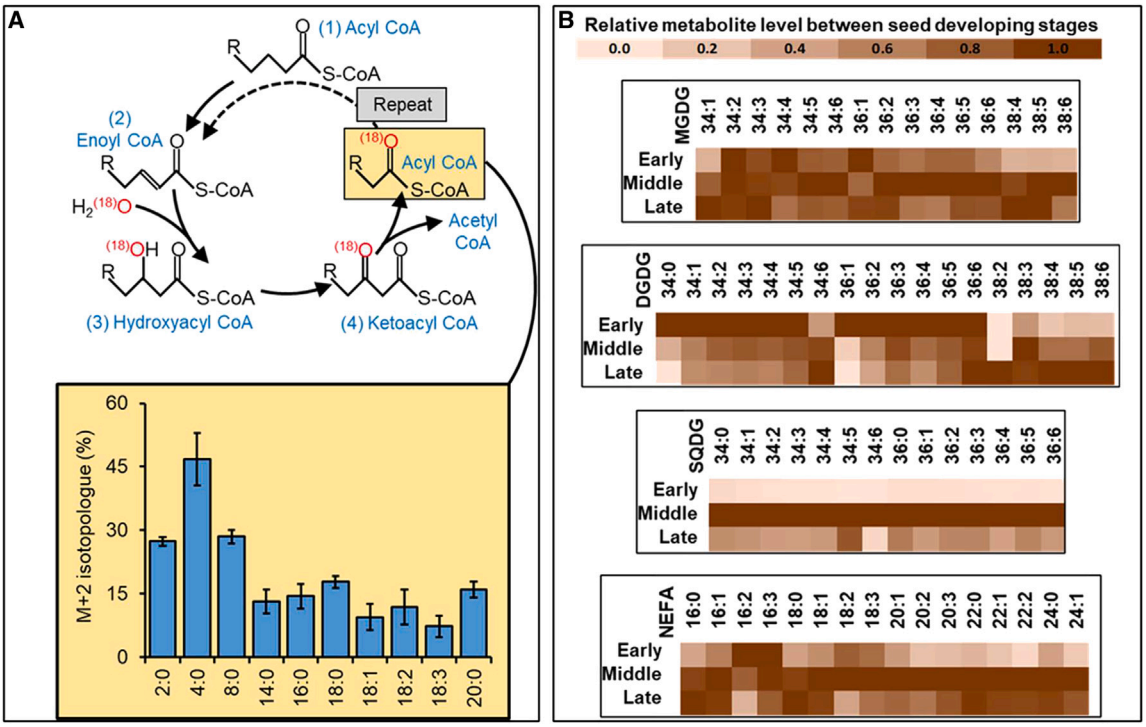

Figure 3. Validation of β-oxidation in oil filling seeds by labeling study and lipidomics

(A) ^{18}O-water labeling of mid-stage camelina seeds for 30 min. Enrichment of M+2 isotopologs are presented (mean ± SD; n = 3).

(B) Relative level of galactolipids (presented as sum of two fatty acids) and non-esterified fatty acids (NEFAs) in developing camelina seeds. Heatmaps show mean values (n = 3). t tests are presented in Data S3. A value of one on the scale bar indicates the largest peak area for a specific lipid across three seed developing stages, with smaller numbers presented as relative values.

^{18}O-water labeling confirms active β-oxidation processes in oil-filling seeds

As breakdown-specific CoAs were abundant in camelina seeds, this tissue was selected for further studies. The presence of short- and medium-chain acyl-CoAs provides conclusive evidence that β-oxidation has occurred at some point during development, but additional evidence is needed to determine when the process was active. Accordingly, we provided ^{18}O-labeled water (50% labeled [w/w]) for 30 min to seeds at the mid-filling stage (20 DPA), when the oil accumulation rate is greatest. Rapid incorporation of ^{18}O resulted in a mass increase by two (M+2) for 4:0, 8:0, and 14:0 acyl-CoAs, consistent with the substitution of ^{18}O for naturally abundant ^{16}O in acyl chains during the β-oxidation process (Figure 3A). In 4:0 acyl-CoA, a common breakdown product of all saturated and unsaturated fatty acids (Figure 1B), the presence of 47% ^{18}O from 50% isotopic water indicated near-complete turnover of the existing short-chain acyl-CoA pool within 30 min and signified active β-oxidation flux. The higher labeling in 4:0 relative to 8:0 reflected the additional breakdown of tri-unsaturated fatty acids, as 4:0 acyl-CoAs can be produced from all forms of unsaturated fatty acids, whereas 8:0 can only be produced from mono- and di-unsaturated substrates (Figure 1B). ^{18}O signatures in longer-chain acyl-CoAs (≥C16) were likely a consequence of isotope incorporation with thioesterase cleavage of acyl-ACPs during biosynthesis.[1,23]

Plastidic galactolipid membranes are turned over as green seeds develop

The breakdown of polyunsaturated fatty acids from lipids was detectable throughout camelina seed development (Figure 2) and supported by changes in the lipid profile (Figure 3B). The presence of 16:1-, 16:2-, and 16:3-containing galactolipids (e.g., 34:4-6 monogalactosyl diacylglycerol [MGDG], digalactosyl diacylglycerol [DGDG], and sulfoquinovosyl diacylglycerol [SQDG]) suggested an active prokaryotic lipid biosynthesis pathway operating in seed filling. However, the abundance of most DGDGs and SQDGs diminished by late development, consistent with lipid breakdown and chloroplast turnover. Pollard and Shachar-Hill[41] quantified biosynthetic rates of combined MGDG and DGDG in mid-filling camelina seeds to be 25 pmol h^{-1} embryo^{-1}, but the level of galactolipids over development was not increased in our study (Figure 3B), thus supporting concomitant plastid lipid breakdown with synthesis. The breakdown of galactolipids in thylakoid membranes is accompanied by chlorophyll remobilization and loss of green hue during senescence and under stress conditions[42]; however, the breakdown of DGDG occurred earlier, when camelina seeds were green, including early and mid-stages of seed development. Possibly the dynamics are associated with maintenance of the photosynthetic complexes, including photosystem II or chloroplast thylakoid turnover.

The presence of unconventional acyl-ACPs (16:1 and 16:3 ACPs), previously reported by our group,[25,43] indicate galactolipid

degradation. These ACPs are not a known part of fatty acid synthesis in plants. Rather, they likely represent membrane lipid hydrolysis by lipases, releasing non-esterified fatty acids (NEFAs), which are then reattached to an ACP backbone.[44] In the present study, long-chain NEFAs, including 16:1, 16:2, and 16:3 NEFAs, were consistently present throughout seed filling. Fatty acid synthesis in chloroplasts and acyl editing in the ER can produce 16:0 and 18/20/22:x acyl chains, respectively, but this does not result in polyunsaturated C16 groups.[36] Conversely, 16:1- to 16:3-containing lipids are produced in chloroplasts by FAD4–8 enzymes but are not thought to undergo acyl editing.[36] Therefore, we infer that the presence of 16:1–16:3 NEFAs must indicate galactolipid degradation. Early in development, the abundance of 16:2 and 16:3 NEFAs matched the high proportion of acyl-CoAs derived from di- and tri-unsaturated fatty acid breakdown (Figure 2). These results suggest that galactolipid degradation, followed by fatty acid oxidation, occurs in green oilseeds starting with early stages of seed filling, although the possibility that some fatty acids were used in lipid remodeling cannot be excluded (Figure S4; Table S1).

Lipid degradation is supported by prior gene expression data. Analysis of available camelina transcriptomics information[45] indicated a plastid lipase 1 homolog that is highly expressed in the early-filling stages, may facilitate the degradation of galactolipids (Figure S5; Data S4). Lipases, including oil body lipase 1 homologs, were also highly expressed at early-filling stages and would support TAG breakdown; however, unlike chloroplast lipids, the degradation of endoplasmic reticulum-based lipids over development could not be definitively established from lipidomics results (Figure S4).

Peroxisomal oxidation capacity during seed filling is comparable to that of germination

We compared fatty acid oxidation in early seed filling with that in germinating seedlings, where β-oxidation is well established. Fatty acid oxidation in plants has been described in the peroxisomes,[32,46] where the acyl-CoA is converted to enoyl-CoA in the first step of β-oxidation catalyzed by ACX (Figure 1A). ACX genes utilize distinct substrates of different chain lengths. ACX1 is specific for long-chain acyl-CoAs (e.g., 16:0), ACX3 utilizes medium chains (e.g., 8:0), and ACX4 acts on short-chain acyl-CoAs (e.g., 4:0).[32] Since both lipidomics and acyl-CoA detection indicated that fatty acid oxidation begins early in seed filling, we examined ACX activity for peroxisomal flux at this stage (Figure 4A), evaluating substrates of different chain lengths. Additionally, 18:3-CoA was used to validate the breakdown of polyunsaturates. The oxidation of long- and short-chain substrates was comparable in both tissues, indicating that the early stages of oil filling had a fatty acid degradation capacity similar to that of germinating seedlings. Medium-chain oxidation activity was elevated in both tissues but more prominent during germination.

We investigated published data[45] on the expression of genes encoding enzymes that could be responsible for early-seed fatty acid oxidation (Figure 4B). Candidates for genetic manipulation to reduce fatty acid breakdown during early oil accumulation in camelina include ACX1, ACX4, KAT1, and KAT5. The homologs of two ketoacyl-CoA thiolases (KAT1 and KAT5) were highly expressed at early-filling stages. Consistent with activity assays, one ACX1 homolog and three ACX4 homologs were higher in abundance and showed higher expression during early seed development. Reduced expression of medium-chain ACXs at early-filling stages compared to germinating seedlings supported the reduced activity for the degradation of 8:0 and 12:0 acyl-CoA substrates. Expression of ACX2, which preferentially uses very long-chain substrates (>20C in acyl-chain), was lower, supporting our hypothesis that elongated fatty acids are possibly more stable as observed in rapeseed (Figure 2).

β-oxidation occurs during both day and night

De novo fatty acid biosynthesis is elevated in light in green tissues, including green oilseeds.[47,48] Conversely, when leaves are exposed to prolonged darkness, genes associated with lipid degradation are expressed,[49,50] implying a circadian alternation of synthesis and breakdown. However, the assumption that fatty acid oxidation does not occur during the day has not been assessed. Because developing seeds stably produce inert storage reserves, including storage lipids, the high lipid concentration may mask evidence of their breakdown during the day. We examined the influence of photoperiod on fatty acid dynamics using a 16-h light (6 a.m. to 10 p.m.)/8-h dark diurnal cycle. Breakdown-specific acyl-CoA levels were elevated during darkness until morning (as expected), reduced at midday, and elevated again in the evening in the last phase of the photoperiod (Figure 5A). The latter two data points suggest that fatty acid breakdown in seeds occurs even in the face of biosynthesis, similar to starch degradation in leaves.[51] We hypothesize that fatty acid breakdown may be part of a homeostatic mechanism to ensure sufficient carbon for seed metabolic activities during the night and reflect the daily supply of photosynthate. Additionally, the trend of acyl-CoA consumption and utilization (Figure 5A) suggests that fatty acid biosynthesis (up to 18 carbons) and lipid desaturation were highest early in the day, but fatty acid elongation (20–22 carbons) increased later in the photoperiod. Similarly, principal-component analysis (PCA) indicated that very-long-chain CoAs (C20–24) had distinct metabolism relative to other CoA esters involved in lipid biosynthesis. Eigenvectors of the PCA aligned with expected metabolic processes (Figure 5B), including elevated synthesis (10 a.m.–2 p.m.) and degradation (2 a.m.–6 a.m.) that differed from a third period (6 p.m.–10 p.m.).

Fatty acid breakdown during the day was further probed with ^{13}C isotopes. Uniformly labeled ^{13}C glucose was provided through an 8-h silique culturing method[53] from 10 a.m. to 6 p.m., corresponding to the central portion of the daytime period. Labeled glucose was metabolized into acetyl-CoA, resulting in ^{13}C-enriched fatty acids within the 8-h labeling period (Figure 5C). Within the same experimental time, ^{13}C was observed in short-chain acyl-CoAs specific to β-oxidation (e.g., 11% ^{13}C-containing 4:0 acyl-CoA after correction for natural ^{13}C abundance). We found that ^{13}C in short-chain acyl-CoAs is only possible when newly produced ^{13}C-labeled lipids or fatty acids undergo β-oxidation, unequivocally demonstrating the concomitant biosynthesis and breakdown of fatty acids. The results implied that breakdown was continuous, not a holdover

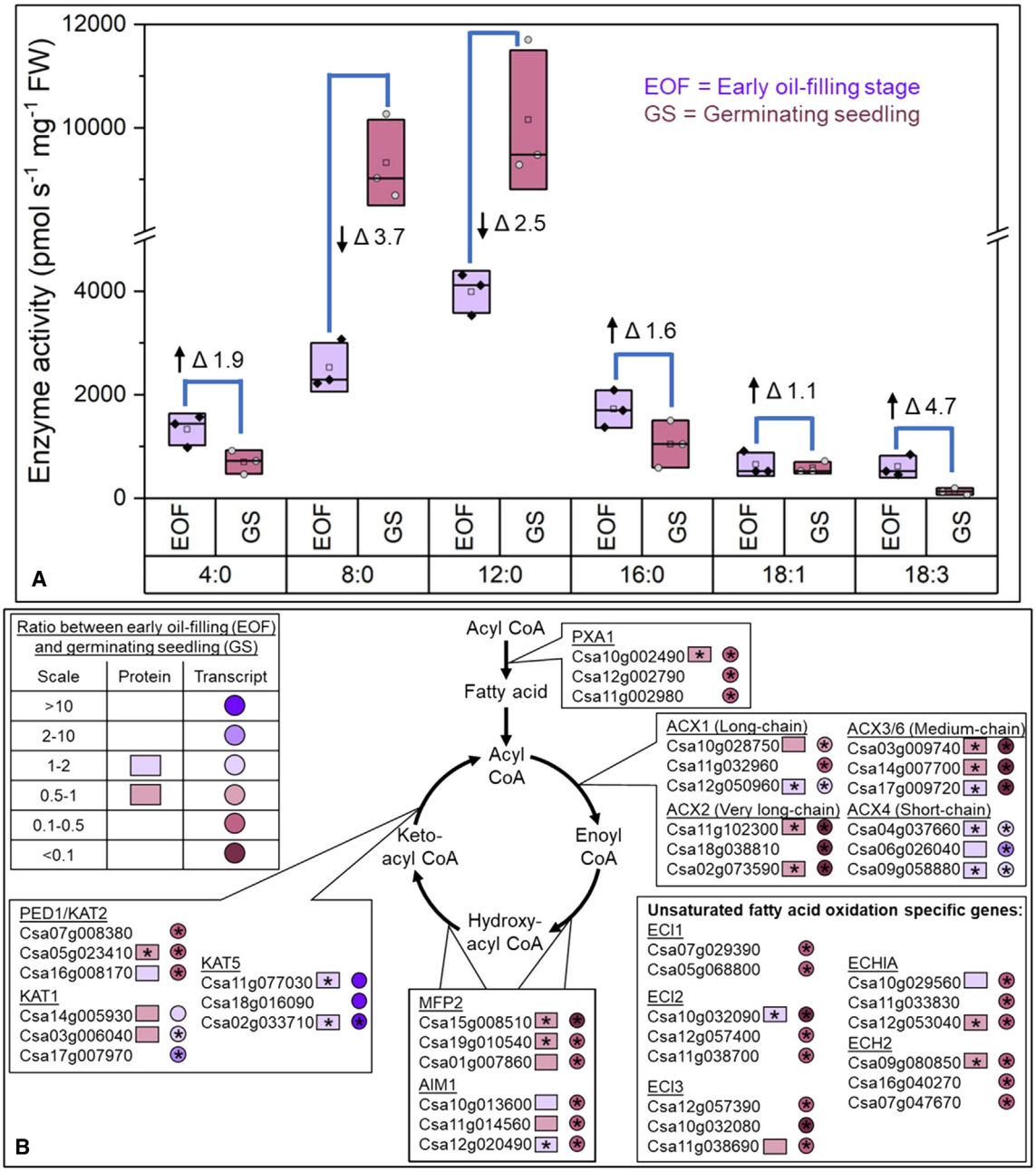

Figure 4. Substantial β-oxidation activity at early-oil filling camelina seeds

(A) Six different substrates, namely 4:0, 8:0, 12:0, 16:0, 18:1, and 18:3 acyl-CoA, were provided in independent assays to assess the activity of different acyl CoA oxidases (ACXs) at EOF seeds and GSs in camelina ($n = 3$).

(B) Comparison of protein and transcript abundances of genes related to fatty acid oxidation between EOF and GS. Omics information is presented in Data S5. Statistical significance (t test) is indicated by an asterisk at $p < 0.05$ ($n = 3$).

from nocturnal metabolism. K-means clustering analysis revealed three different distinct clusters based on ^{13}C description (Figure 5C). The first class consisted of less labeled acyl-CoAs, mostly with specific signatures for β-oxidation (C4–14) and galactolipid breakdown (16:1/2/3), consistent with lipidomics data (Figure 3B). Since 4:0-acyl-CoA was at near-isotopic equilibrium by 30 min in the ^{18}O-labeling study (Figure 3A), the slower labeling of this pool in the ^{13}C study indicated that fatty acid degradation included preexisting unlabeled lipids in addition to newly synthesized acyl chains. Highly labeled second and third clusters consisted of mostly synthesis-specific CoAs. Compared to 18:1 acyl-CoA, 18:2 and 18:3 belonged to the less-labeled

A

Scale bar

1.00
0.80
0.60
0.40
0.20
0.00

Fatty acid and lipid breakdown-specific CoAs

	4:0	6:0	8:0	10:0	12:0	14:0	10:1	14:2	16:1	16:2	16:3
02:00 h	0.43	1.00	1.00	0.87	0.27	0.50	0.30	0.39	0.36	0.47	0.42
06:00 h	0.64	0.52	0.61	1.00	0.42	1.00	1.00	0.64	0.69	0.78	0.40
10:00 h	1.00	0.61	0.25	1.00	1.00	0.89	0.99	1.00	1.00	1.00	1.00
14:00 h	0.13	0.38	0.09	0.12	0.12	0.35	0.08	0.09	0.56	0.42	0.84
18:00 h	0.54	0.63	0.32	0.41	0.24	0.42	0.37	0.34	0.39	0.50	0.26
22:00 h	0.41	0.36	0.64	0.23	0.20	0.35	0.16	0.19	0.17	0.26	0.13

Photoperiod

	En-10:1	Dien-10:1	En-12:1	En-12:2	En-14:0	En-14:1	En-14:2	En-18:3	Ke-4:0	Ke-8:0	Ke-10:0	Ke-14:0	Ke-18:0
02:00 h	0.49	1.00	0.94	1.00	0.48	0.39	0.48	0.53	0.48	0.93	1.00	0.22	0.63
06:00 h	1.00	0.78	0.95	0.93	1.00	0.52	0.53	0.40	0.83	0.54	0.78	0.56	0.88
10:00 h	0.28	0.70	1.00	0.89	0.47	1.00	1.00	1.00	1.00	1.00	0.77	1.00	1.00
14:00 h	0.02	0.19	0.24	0.38	0.17	0.11	0.24	0.56	0.64	0.23	0.27	0.09	0.17
18:00 h	0.13	0.33	0.73	0.82	0.31	0.32	0.73	0.49	0.42	0.27	0.59	0.46	0.48
22:00 h	0.14	0.29	0.50	0.54	0.32	0.26	0.41	0.24	0.61	0.40	0.62	0.19	0.24

Fatty acid and lipid biosynthesis-specific CoAs

	2:0	16:0	18:0	18:1	18:2	18:3	20:0	20:1	22:0	22:1	24:0	24:1	Ke-20:0
02:00 h	0.52	0.87	0.57	0.46	0.36	0.58	1.00	0.94	1.00	1.00	1.00	1.00	0.14
06:00 h	1.00	0.81	0.63	1.00	0.61	0.41	0.70	1.00	0.68	0.67	0.64	0.48	0.28
10:00 h	0.90	1.00	1.00	0.92	0.92	1.00	0.04	0.20	0.06	0.04	0.05	0.05	1.00
14:00 h	0.08	0.49	0.51	0.30	1.00	0.91	0.06	0.08	0.09	0.05	0.02	0.02	0.48
18:00 h	0.49	0.62	0.71	0.50	0.35	0.54	0.06	0.22	0.07	0.06	0.07	0.10	0.11
22:00 h	0.39	0.45	0.92	0.19	0.16	0.26	0.23	0.24	0.20	0.18	0.26	0.27	0.10

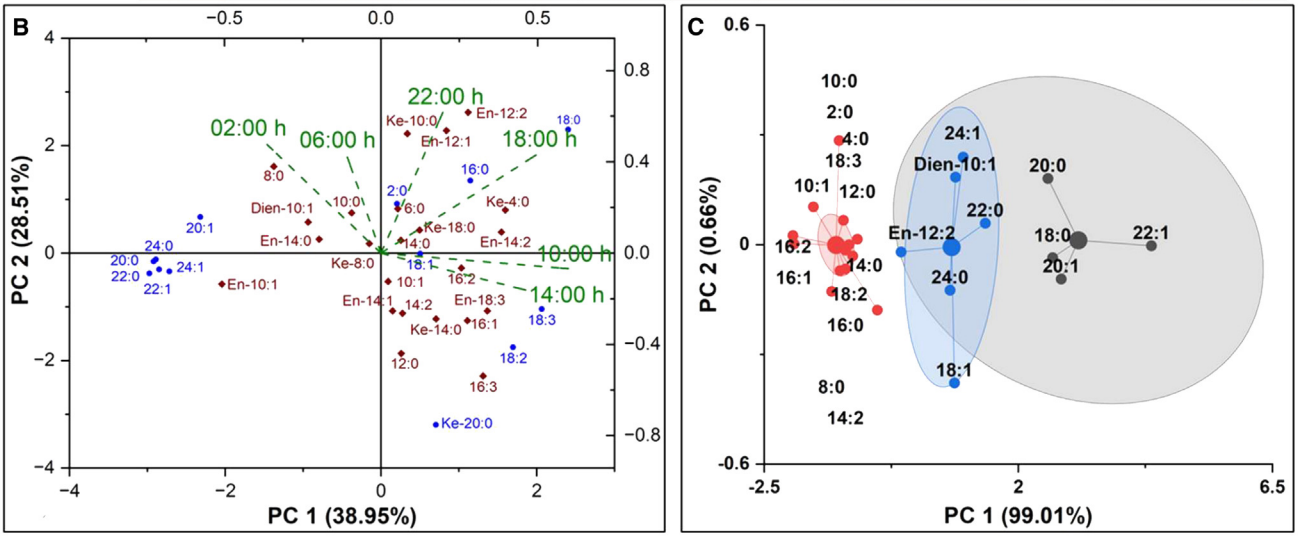

Figure 5. Dynamic fatty acid metabolism over the photoperiod in the middle stage of seed filling in camelina

(A) Heatmap and (B) PCA of relative acyl-CoA abundance in each 4-h window during light (6 a.m.–10 p.m.) and dark (10 p.m.–6 a.m.) periods to visualize acyl-CoA changes over 24 h, and clusters of acyl-CoAs and time points. A value of one on the scale bar of the heatmap indicates the largest peak area for a specific CoA across six time points, with smaller numbers presented as relative values. Blue, dark red, and green colors denote synthesis-specific CoAs, breakdown-specific CoAs, and the time of photoperiod, respectively.

(C) k-Means clustering analysis of the ^{13}C-touched pool fraction[52] from 8 h of silique culturing in U-$^{13}C_6$ glucose media. $n = 3$ for all three figures. Red, blue, and gray groups represent low, medium, and high ^{13}C-incorporation groups, respectively.

cluster, suggesting that less fatty acid desaturation on phosphatidylcholine (PC) occurs during the experimental period of mid- to late photoperiod. Together with this result, a continuous increase of polyunsaturates in abundance in the early light hours, but later decreasing (Figure 5A), suggests that desaturation events occur mostly in the late night to early morning, supporting previous observations in Arabidopsis leaves.[54] Furthermore, isotope incorporation into 12:2-enoyl- and 10:1-dienoyl-CoA indicated a breakdown of newly formed polyunsaturated fatty acids throughout the day and further confirmed the breakdown of lipids as the polyunsaturates are only produced on a lipid backbone (Figure 1).

β-oxidation is a target for engineering

Our discovery of fatty acid breakdown in multiple tissues suggests that previous engineering efforts may have been

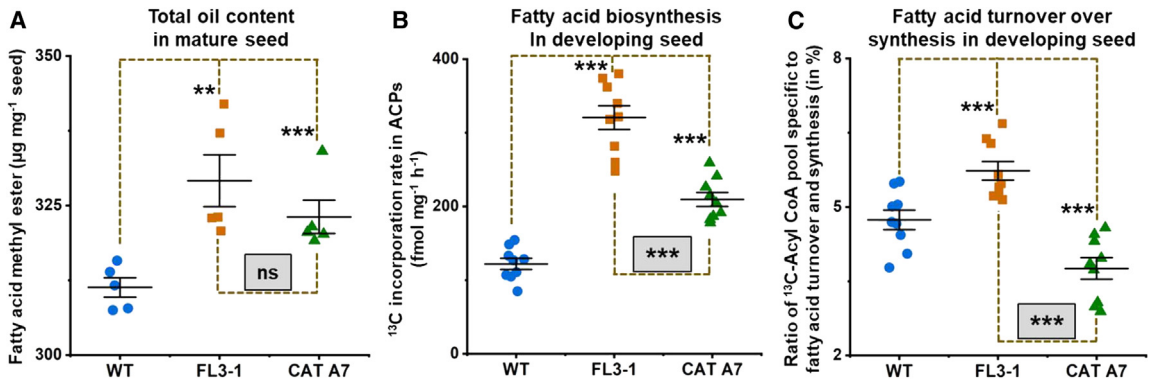

Figure 6. Changes in dynamic fatty acid metabolism in engineered camelina lines

(A) Total oil content at maturity based on quantification of fatty acid methyl esters (n = 5), (B) relative biosynthesis rate at mid-seed filling by measuring ^{13}C ACP pools (n = 9), and (C) percent breakdown of synthesized fatty acids at mid-seed filling by comparing ^{13}C pools of synthesis-specific long-chain acyl-CoAs (16:0, 18:0, and 18:1) with breakdown-specific short-chain acyl-CoAs (4:0, 8:0, and 10:0) (n = 9) were determined in wild type (WT) and two transgenic lines (FL3-1 and CAT A7) (Data S6). Data are represented as mean ± SE. Statistical significance (t tests) is indicated by **p < 0.03; ***p < 0.01; and ns, no statistical difference at p = 0.05.

thwarted by mechanisms that induce lipid breakdown when plants are altered to produce more oil, perhaps a component of homeostasis. We evaluated this hypothesis by examining seeds from high-oil engineered camelina lines. Wild-type camelina plants were compared to two transgenic lines with enhanced levels of a α-carboxyltransferase subunit of the acetyl-CoA carboxylase (ACCase) enzyme complex, full-length (FL3-1) and catalytic (CAT A7) lines,[4] that resulted in higher amounts of seed oil (Figure 6A). Using ^{13}C-labeling, isotope incorporation into acyl-ACPs[25,52] and acyl-CoAs was measured to compare rates of fatty acid synthesis and breakdown, respectively. Both engineered lines produced statistically similar amounts of lipids in their mature seeds (Figure 6A); however, the FL3-1 line showed higher rates of fatty acid biosynthesis (Figure 6B) and breakdown (Figure 6C). Similarly, a recent study from our group in Arabidopsis showed the increased proteins and transcripts of various peroxisomal oxidation genes when the flux through the *de novo* fatty acid biosynthetic pathway increased in the double mutant of biotin attachment domain-containing proteins, which negatively regulates ACCase.[55] We postulate that altered synthesis and breakdown rates could help keep free fatty acids levels in check that would otherwise become toxic to the cell.[12,17]

Evaluation of the transgenics suggested oil accumulation might have been higher if it had not been limited by concomitant breakdown of fatty acids. The FL3-1 line showed increased lipid levels accompanied by both the highest synthesis and breakdown rates, while CAT A7 line showed elevated lipid levels due to synthesis rates higher than the WT (but lower than the FL3-1 line) combined with the lowest degradation rates. These results indicate that reducing the degree of β-oxidation may contribute to achieving higher lipid levels. We estimated that approximately 4%–6% of newly synthesized fatty acids were continuously turned over at the peak of seed filling in WT during the daytime. As higher degradation rates at night (Figure 5A) and enhanced breakdown with early and late filling stages (Figure 2) are not considered, this is a conservative estimate. Lipids are continuously broken down to repurpose acyl chains as in membrane remodeling that responds to environment or TAG remodeling.[56] In addition, the present study mechanistically describes β-oxidation of fatty acids, which can have a significant impact on the seed carbon economy and thereby impact development of future oil-rich crops. Our data suggest a reconsideration of prevailing assumptions that sink metabolism in seeds is inherently "stable," with implications for breeding and engineering efforts.

Limitations of the study

In the present study, we examined developing seeds of camelina and rapeseed and a tobacco line engineered to produce high levels of lipids in leaves. Although our results suggest that lipid oxidation occurs broadly in plant tissues over multiple stages of development, this is a generalization and may not be the case in all systems, especially those producing less oil. Extending investigations into additional species in the future will more definitively establish the extent of this phenomenon. Furthermore, the controlled experimental conditions in this study may not faithfully reflect environmental factors in the field, such as changes in light intensity, temperature, or nutrient availability. We hypothesize that oxidation would be elevated in a number of perturbed conditions; however, this remains to be established. Finally, the present study highlights the increased degradation of fatty acids by engineered plants, but it does not attempt to elucidate the regulatory mechanisms that lead to increased catabolism, leaving gaps in our understanding of this important process, with biotechnological implications for future renewable fuels production.

RESOURCE AVAILABILITY

Lead contact

Further information and requests for resources and reagents should be directed to and will be fulfilled by the lead contact, Doug K. Allen (doug.allen@ars.usda.gov).

Materials availability

This study did not generate new unique reagents.

Data and code availability

All data needed to evaluate the conclusions in the paper are present in the paper and/or the supplemental information. Files that include CoA quantification, labeling measurements in acyl-CoA and acyl-ACP, and fatty acyl methyl ester measurements and lipidomics have been deposited in the Zenodo public repository and are publicly available (DOI and Zenodo Data: https://doi.org/10.5281/zenodo.14393795; https://doi.org/10.5281/zenodo.14396946). This study did not generate any code. Any additional information required to reanalyze the data reported in this paper is available from the lead contact upon request.

ACKNOWLEDGMENTS

We thank Dr. Tony Larson (University of York) for providing insights into the acyl-CoA method development. We acknowledge the Plant Growth Facility at Donald Danforth Plant Science Center for assistance with plant growth and maintenance. We thank Dr. Xue-Rong Zhou from the Commonwealth Scientific and Industrial Research Organisation (Australia) for providing the transgenic tobacco lines and Sally Bailey (Donald Danforth Plant Science Center) for technical assistance with measuring ACPs. Liquid chromatography (LC)-MS data were acquired in the Bioanalytical Chemistry Facility of the Donald Danforth Plant Science Center. The authors greatly appreciate helpful feedback from Drs. Elizabeth (Toby) A. Kellogg, Ian (Max) Moller, Edgar B. Cahoon, and Philip D. Bates. This work was supported by National Science Foundation grant no. IOS-1829365, National Science Foundation grant no. MCB-2242822, US Department of Energy Office of Science, Office of Biological and Environmental Research grant no. DE-SC0023142, US Department of Energy Office of Science, Office of Biological and Environmental Research grant no. DE-SC0022207, US Department of Agriculture-National Institute of Food and Agriculture grant no. 2021-67013-33778, US Department of Agriculture-National Institute of Food and Agriculture grant no. 2023-67017-39419, US Department of Agriculture-Agricultural Research Service (USDA-ARS), and the Subterranean Influences on Nitrogen and Carbon (SINC) Center at Donald Danforth Plant Science Center.

AUTHOR CONTRIBUTIONS

Conceptualization: S.K. and D.K.A.; methodology: S.K., R.B.W., and D.K.A.; investigation: S.K., P.J., M.L., C.X., M.W., and K.L.C.; visualization: S.K. and D.K.A.; funding acquisition: A.J.K., J.J.T., D.X., and D.K.A.; project administration: A.J.K., J.J.T., D.X., and D.K.A.; supervision: S.K. and D.K.A.; writing – original draft: S.K. and D.K.A.; writing – review & editing: S.K., P.J., M.L., C.X., M.W., K.L.C., R.B.W., A.J.K., J.J.T., D.X., and D.K.A.

DECLARATION OF INTERESTS

The authors declare no competing interests.

STAR★METHODS

Detailed methods are provided in the online version of this paper and include the following:

SUPPLEMENTAL INFORMATION

Supplemental information can be found online at https://doi.org/10.1016/j.celrep.2025.115492.

Received: July 26, 2024
Revised: February 3, 2025
Accepted: March 10, 2025
Published: March 29, 2025

REFERENCES

1. Allen, D.K., Bates, P.D., and Tjellström, H. (2015). Tracking the metabolic pulse of plant lipid production with isotopic labeling and flux analyses: Past, present and future. Prog. Lipid Res. *58*, 97–120. https://doi.org/10.1016/j.plipres.2015.02.002.
2. Durrett, T.P., Benning, C., and Ohlrogge, J. (2008). Plant triacylglycerols as feedstocks for the production of biofuels. Plant J. *54*, 593–607. https://doi.org/10.1111/j.1365-313X.2008.03442.x.
3. Singh, R., Arora, A., and Singh, V. (2021). Biodiesel from oil produced in vegetative tissues of biomass – A review. Bioresour. Technol. *326*, 124772. https://doi.org/10.1016/j.biortech.2021.124772.
4. Wang, M., Garneau, M.G., Poudel, A.N., Lamm, D., Koo, A.J., Bates, P.D., and Thelen, J.J. (2022). Overexpression of pea α-carboxyltransferase in Arabidopsis and camelina increases fatty acid synthesis leading to improved seed oil content. Plant J. *110*, 1035–1046. https://doi.org/10.1111/tpj.15721.
5. Pelletier, J.M., Kwong, R.W., Park, S., Le, B.H., Baden, R., Cagliari, A., Hashimoto, M., Munoz, M.D., Fischer, R.L., Goldberg, R.B., and Harada, J.J. (2017). LEC1 sequentially regulates the transcription of genes involved in diverse developmental processes during seed development. Proc. Natl. Acad. Sci. *114*, E6710–E6719. https://doi.org/10.1073/pnas.1707957114.
6. Song, J., Xie, X., Chen, C., Shu, J., Thapa, R.K., Nguyen, V., Bian, S., Kohalmi, S.E., Marsolais, F., Zou, J., and Cui, Y. (2021). LEAFY COTYLEDON1 expression in the endosperm enables embryo maturation in Arabidopsis. Nat. Commun. *12*, 3963. https://doi.org/10.1038/s41467-021-24234-1.
7. Park, K., Quach, T., Clark, T.J., Kim, H., Zhang, T., Wang, M., Guo, M., Sato, S., Nazarenus, T.J., Blume, R., et al. (2025). Development of vegetative oil sorghum: From lab-to-field. Plant Biotechnol. J. *23*, 660–673. https://doi.org/10.1111/pbi.14527.
8. Morley, S.A., Ma, F., Alazem, M., Frankfater, C., Yi, H., Burch-Smith, T., Clemente, T.E., Veena, V., Nguyen, H., and Allen, D.K. (2023). Expression of malic enzyme reveals subcellular carbon partitioning for storage reserve production in soybeans. New Phytol. *239*, 1834–1851. https://doi.org/10.1111/nph.18835.
9. Mukherjee, T., Kambhampati, S., Morley, S.A., Durrett, T.P., and Allen, D.K. (2025). Metabolic flux analysis to increase oil in seeds. Plant Physiol. *197*, kiae595. https://doi.org/10.1093/plphys/kiae595.
10. Chia, T.Y.P., Pike, M.J., and Rawsthorne, S. (2005). Storage oil breakdown during embryo development of Brassica napus (L.). J. Exp. Bot. *56*, 1285–1296. https://doi.org/10.1093/jxb/eri129.
11. Kambhampati, S., Aznar-Moreno, J.A., Bailey, S.R., Arp, J.J., Chu, K.L., Bilyeu, K.D., Durrett, T.P., and Allen, D.K. (2021). Temporal changes in metabolism late in seed development affect biomass composition. Plant Physiol. *186*, 874–890. https://doi.org/10.1093/plphys/kiab116.
12. Poirier, Y., Ventre, G., and Caldelari, D. (1999). Increased Flow of Fatty Acids toward β-Oxidation in Developing Seeds of Arabidopsis Deficient in Diacylglycerol Acyltransferase Activity or Synthesizing Medium-Chain-Length Fatty Acids1. Plant Physiol. *121*, 1359–1366. https://doi.org/10.1104/pp.121.4.1359.

13. Wilson, R.F., and Rinne, R.W. (1976). Studies on lipid synthesis and degradation in developing soybean cotyledons. Plant Physiol. *57*, 375–381. https://doi.org/10.1104/pp.57.3.375.

14. Moire, L., Rezzonico, E., Goepfert, S., and Poirier, Y. (2004). Impact of Unusual Fatty Acid Synthesis on Futile Cycling through β-Oxidation and on Gene Expression in Transgenic Plants. Plant Physiol. *134*, 432–442. https://doi.org/10.1104/pp.103.032938.

15. Froman, B.E., Edwards, P.C., Bursch, A.G., and Dehesh, K. (2000). ACX3, a Novel Medium-Chain Acyl-Coenzyme A Oxidase from Arabidopsis. Plant Physiol. *123*, 733–742. https://doi.org/10.1104/pp.123.2.733.

16. Gerhardt, B. (1983). Localization of β-oxidation enzymes in peroxisomes isolated from nonfatty plant tissues. Planta *159*, 238–246. https://doi.org/10.1007/BF00397531.

17. Eccleston, V., and Ohlrogge, J. (1998). Expression of lauroyl-acyl carrier protein thioesterase in brassica napus seeds induces pathways for both fatty acid oxidation and biosynthesis and implies a set point for triacylglycerol accumulation. Plant Cell *10*, 613–622. https://doi.org/10.1105/tpc.10.4.613.

18. Hou, Q., Ufer, G., and Bartels, D. (2016). Lipid signalling in plant responses to abiotic stress. Plant Cell Environ. *39*, 1029–1048. https://doi.org/10.1111/pce.12666.

19. Yu, L., Zhou, C., Fan, J., Shanklin, J., and Xu, C. (2021). Mechanisms and functions of membrane lipid remodeling in plants. Plant J. *107*, 37–53. https://doi.org/10.1111/tpj.15273.

20. Goepfert, S., and Poirier, Y. (2007). β-Oxidation in fatty acid degradation and beyond. Curr. Opin. Plant Biol. *10*, 245–251. https://doi.org/10.1016/j.pbi.2007.04.007.

21. Graham, I.A., and Eastmond, P.J. (2002). Pathways of straight and branched chain fatty acid catabolism in higher plants. Prog. Lipid Res. *41*, 156–181. https://doi.org/10.1016/S0163-7827(01)00022-4.

22. Koley, S., Jyoti, P., Lingwan, M., and Allen, D.K. (2024). Isotopically nonstationary metabolic flux analysis of plants: recent progress and future opportunities. New Phytol. *242*, 1911–1918. https://doi.org/10.1111/nph.19734.

23. Allen, D.K. (2016). Assessing compartmentalized flux in lipid metabolism with isotopes. Biochim. Biophys. Acta *1861*, 1226–1242. https://doi.org/10.1016/j.bbalip.2016.03.017.

24. Dyer, J.M., Stymne, S., Green, A.G., and Carlsson, A.S. (2008). High-value oils from plants. Plant J. *54*, 640–655. https://doi.org/10.1111/j.1365-313X.2008.03430.x.

25. Nam, J.-W., Jenkins, L.M., Li, J., Evans, B.S., Jaworski, J.G., and Allen, D.K. (2020). A General Method for Quantification and Discovery of Acyl Groups Attached to Acyl Carrier Proteins in Fatty Acid Metabolism Using LC-MS/MS. Plant Cell *32*, 820–832. https://doi.org/10.1105/tpc.19.00954.

26. Ohlrogge, J.B., Kuhn, D.N., and Stumpf, P.K. (1979). Subcellular localization of acyl carrier protein in leaf protoplasts of Spinacia oleracea. Proc. Natl. Acad. Sci. *76*, 1194–1198. https://doi.org/10.1073/pnas.76.3.1194.

27. Knoop, F. (1904). Der Abbau aromatischer fettsäuren im tierkörper. Beitr. Chem. Physiol. Pathol. *6*, 150–162.

28. Cooper, T.G., and Beevers, H. (1969). β Oxidation in Glyoxysomes from Castor Bean Endosperm. J. Biol. Chem. *244*, 3514–3520. https://doi.org/10.1016/S0021-9258(18)83402-0.

29. Hayashi, H., De Bellis, L., Ciurli, A., Kondo, M., Hayashi, M., and Nishimura, M. (1999). A Novel Acyl-CoA Oxidase That Can Oxidize Short-chain Acyl-CoA in Plant Peroxisomes. J. Biol. Chem. *274*, 12715–12721. https://doi.org/10.1074/jbc.274.18.12715.

30. Pinfield-Wells, H., Rylott, E.L., Gilday, A.D., Graham, S., Job, K., Larson, T.R., and Graham, I.A. (2005). Sucrose rescues seedling establishment but not germination of Arabidopsis mutants disrupted in peroxisomal fatty acid catabolism. Plant J. *43*, 861–872. https://doi.org/10.1111/j.1365-313X.2005.02498.x.

31. Rylott, E.L., Rogers, C.A., Gilday, A.D., Edgell, T., Larson, T.R., and Graham, I.A. (2003). Arabidopsis Mutants in Short- and Medium-chain Acyl-CoA Oxidase Activities Accumulate Acyl-CoAs and Reveal That Fatty Acid β-Oxidation Is Essential for Embryo Development. J. Biol. Chem. *278*, 21370–21377. https://doi.org/10.1074/jbc.M300826200.

32. Adham, A.R., Zolman, B.K., Millius, A., and Bartel, B. (2005). Mutations in Arabidopsis acyl-CoA oxidase genes reveal distinct and overlapping roles in beta-oxidation. Plant J. *41*, 859–874. https://doi.org/10.1111/j.1365-313X.2005.02343.x.

33. Goepfert, S., Vidoudez, C., Rezzonico, E., Hiltunen, J.K., and Poirier, Y. (2005). Molecular identification and characterization of the Arabidopsis delta (3,5), delta (2,4)-dienoyl-coenzyme A isomerase, a peroxisomal enzyme participating in the beta-oxidation cycle of unsaturated fatty acids. Plant Physiol. *138*, 1947–1956. https://doi.org/10.1104/pp.105.064311.

34. Poirier, Y., Antonenkov, V.D., Glumoff, T., and Hiltunen, J.K. (2006). Peroxisomal β-oxidation—A metabolic pathway with multiple functions. Biochim. Biophys. Acta *1763*, 1413–1426. https://doi.org/10.1016/j.bbamcr.2006.08.034.

35. Gerhardt, B. (1992). Fatty acid degradation in plants. Prog. Lipid Res. *31*, 417–446. https://doi.org/10.1016/0163-7827(92)90004-3.

36. Li-Beisson, Y., Shorrosh, B., Beisson, F., Andersson, M.X., Arondel, V., Bates, P.D., Baud, S., Bird, D., DeBono, A., Durrett, T.P., et al. (2013). Acyl-Lipid Metabolism. Arabidopsis Book *11*, e0161. https://doi.org/10.1199/tab.0161.

37. Larson, T.R., and Graham, I.A. (2001). Technical Advance: a novel technique for the sensitive quantification of acyl CoA esters from plant tissues. Plant J. *25*, 115–125. https://doi.org/10.1046/j.1365-313x.2001.00929.x.

38. Vanhercke, T., El Tahchy, A., Liu, Q., Zhou, X.-R., Shrestha, P., Divi, U.K., Ral, J.-P., Mansour, M.P., Nichols, P.D., James, C.N., et al. (2014). Metabolic engineering of biomass for high energy density: oilseed-like triacylglycerol yields from plant leaves. Plant Biotechnol. J. *12*, 231–239. https://doi.org/10.1111/pbi.12131.

39. Johnson, B.S., Allen, D.K., and Bates, P.D. (2025). Triacylglycerol stability limits futile cycles and inhibition of carbon capture in oil-accumulating leaves. Plant Physiol. *197*, kiae121. https://doi.org/10.1093/plphys/kiae121.

40. Vanhercke, T., Divi, U.K., El Tahchy, A., Liu, Q., Mitchell, M., Taylor, M.C., Eastmond, P.J., Bryant, F., Mechanicos, A., Blundell, C., et al. (2017). Step changes in leaf oil accumulation via iterative metabolic engineering. Metab. Eng. *39*, 237–246. https://doi.org/10.1016/j.ymben.2016.12.007.

41. Pollard, M., and Shachar-Hill, Y. (2022). Kinetic complexities of triacylglycerol accumulation in developing embryos from Camelina sativa provide evidence for multiple biosynthetic systems. J. Biol. Chem. *298*, 101396. https://doi.org/10.1016/j.jbc.2021.101396.

42. Kuai, B., Chen, J., and Hörtensteiner, S. (2018). The biochemistry and molecular biology of chlorophyll breakdown. J. Exp. Bot. *69*, 751–767. https://doi.org/10.1093/jxb/erx322.

43. Jenkins, L.M., Nam, J.-W., Evans, B.S., and Allen, D.K. (2021). Quantification of Acyl-Acyl Carrier Proteins for Fatty Acid Synthesis Using LC-MS/MS. Methods Mol. Biol. *2295*, 219–247. https://doi.org/10.1007/978-1-0716-1362-7_13.

44. Koo, A.J.K., Fulda, M., Browse, J., and Ohlrogge, J.B. (2005). Identification of a plastid acyl-acyl carrier protein synthetase in Arabidopsis and its role in the activation and elongation of exogenous fatty acids. Plant J. *44*, 620–632. https://doi.org/10.1111/j.1365-313X.2005.02553.x.

45. Barreda, L., Brosse, C., Boutet, S., Klewko, N., De Vos, D., Francois, T., Collet, B., Grain, D., Boulard, C., Totozafy, J.C., et al. (2025). Multi-omic analyses unveil contrasting composition and spatial distribution of specialized metabolites in seeds of Camelina sativa and other Brassicaceae. Plant J. *121*, e17231. https://doi.org/10.1111/tpj.17231.

46. Zolman, B.K., Martinez, N., Millius, A., Adham, A.R., and Bartel, B. (2008). Identification and characterization of Arabidopsis indole-3-butyric acid

response mutants defective in novel peroxisomal enzymes. Genetics *180*, 237–251. https://doi.org/10.1534/genetics.108.090399.

47. Ruuska, S.A., Schwender, J., and Ohlrogge, J.B. (2004). The Capacity of Green Oilseeds to Utilize Photosynthesis to Drive Biosynthetic Processes. Plant Physiol. *136*, 2700–2709. https://doi.org/10.1104/pp.104.047977.
48. Ohlrogge, J.B., and Jaworski, J.G. (1997). Regulation of Fatty Acid Synthesis. Annu. Rev. Plant Physiol. Plant Mol. Biol. *48*, 109–136. https://doi.org/10.1146/annurev.arplant.48.1.109.
49. Bläsing, O.E., Gibon, Y., Günther, M., Höhne, M., Morcuende, R., Osuna, D., Thimm, O., Usadel, B., Scheible, W.-R., and Stitt, M. (2005). Sugars and Circadian Regulation Make Major Contributions to the Global Regulation of Diurnal Gene Expression in Arabidopsis. Plant Cell *17*, 3257–3281. https://doi.org/10.1105/tpc.105.035261.
50. Rosenwasser, S., Rot, I., Sollner, E., Meyer, A.J., Smith, Y., Leviatan, N., Fluhr, R., and Friedman, H. (2011). Organelles Contribute Differentially to Reactive Oxygen Species-Related Events during Extended Darkness. Plant Physiol. *156*, 185–201. https://doi.org/10.1104/pp.110.169797.
51. Fernandez, O., Ishihara, H., George, G.M., Mengin, V., Flis, A., Sumner, D., Arrivault, S., Feil, R., Lunn, J.E., Zeeman, S.C., et al. (2017). Leaf Starch Turnover Occurs in Long Days and in Falling Light at the End of the Day. Plant Physiol. *174*, 2199–2212. https://doi.org/10.1104/pp.17.00601.
52. Chu, K.L., Koley, S., Jenkins, L.M., Bailey, S.R., Kambhampati, S., Foley, K., Arp, J.J., Morley, S.A., Czymmek, K.J., Bates, P.D., and Allen, D.K. (2022). Metabolic flux analysis of the non-transitory starch tradeoff for lipid production in mature tobacco leaves. Metab. Eng. *69*, 231–248. https://doi.org/10.1016/j.ymben.2021.12.003.
53. Koley, S., Chu, K.L., Mukherjee, T., Morley, S.A., Klebanovych, A., Czymmek, K.J., and Allen, D.K. (2022). Metabolic synergy in Camelina reproductive tissues for seed development. Sci. Adv. *8*, eabo7683. https://doi.org/10.1126/sciadv.abo7683.
54. Maatta, S., Scheu, B., Roth, M.R., Tamura, P., Li, M., Williams, T.D., Wang, X., and Welti, R. (2012). Levels of Arabidopsis thaliana Leaf Phosphatidic Acids, Phosphatidylserines, and Most Trienoate-Containing Polar Lipid Molecular Species Increase during the Dark Period of the Diurnal Cycle. Front. Plant Sci. *3*, 49. https://doi.org/10.3389/fpls.2012.00049.
55. Kataya, A., Nascimento, J.R.S., Xu, C., Garneau, M.G., Koley, S., Kimberlin, A., Mooney, B.P., Allen, D.K., Bates, P.D., Koo, A.J., et al. (2023). Comparative omics reveals unanticipated metabolic rearrangements in a high-oil mutant of plastid acetyl-CoA carboxylase. Preprint at: bioRxiv. https://doi.org/10.1101/2023.08.31.555777
56. Parchuri, P., Bhandari, S., Azeez, A., Chen, G., Johnson, K., Shockey, J., Smertenko, A., and Bates, P.D. (2024). Identification of triacylglycerol remodeling mechanism to synthesize unusual fatty acid containing oils. Nat. Commun. *15*, 3547. https://doi.org/10.1038/s41467-024-47995-x.
57. Haslam, R.P., and Larson, T.R. (2021). Techniques for the Measurement of Molecular Species of Acyl-CoAAcyl-CoA in Plants and MicroalgaeMicroalgae. In Plant Lipids: Methods and Protocols Methods in Molecular Biology, D. Bartels and P. Dörmann, eds. (Springer US), pp. 203–218. https://doi.org/10.1007/978-1-0716-1362-7_12.
58. Pearce, R.W., Kodger, J.V., and Sandlers, Y.I. (2022). A liquid chromatography tandem mass spectrometry method for a semiquantitative screening of cellular acyl-CoA. Anal. Biochem. *640*, 114430. https://doi.org/10.1016/j.ab.2021.114430.
59. Li, Y., Beisson, F., Pollard, M., and Ohlrogge, J. (2006). Oil content of Arabidopsis seeds: The influence of seed anatomy, light and plant-to-plant variation. Phytochemistry *67*, 904–915. https://doi.org/10.1016/j.phytochem.2006.02.015.
60. Hummel, J., Segu, S., Li, Y., Irgang, S., Jueppner, J., and Giavalisco, P. (2011). Ultra performance liquid chromatography and high resolution mass spectrometry for the analysis of plant lipids. Front. Plant Sci. *2*, 54. https://doi.org/10.3389/fpls.2011.00054.
61. Tello-Ruiz, M.K., Jaiswal, P., and Ware, D. (2022). Gramene: A Resource for Comparative Analysis of Plants Genomes and Pathways. Methods Mol. Biol. *2443*, 101–131. https://doi.org/10.1007/978-1-0716-2067-0_5.
62. Berardini, T.Z., Reiser, L., Li, D., Mezheritsky, Y., Muller, R., Strait, E., and Huala, E. (2015). The Arabidopsis information resource: Making and mining the "gold standard" annotated reference plant genome. Genesis 2000 *53*, 474–485. https://doi.org/10.1002/dvg.22877.

STAR★METHODS

KEY RESOURCES TABLE

REAGENT or RESOURCE	SOURCE	IDENTIFIER
Chemicals, peptides, and recombinant proteins		
U-$^{13}C_6$ glucose	Cambridge Isotope Laboratories	CLM-1396
^{18}O water	Sigma	329878
$^{13}C_3$ acyl-CoA	Sigma	655759
$^{13}C_{16}$ acyl-CoA	Sigma	655716
Methanol	Fisher Scientific	60-009-55
Methyl *tert*-butyl ether	Sigma	34875
UltimateSPLASH ONE mix	Avanti Polar Lipids	330820
Ammonium acetate	Sigma	238074
Acetic acid	Sigma	AX0074
Acetonitrile	MedSupply Partners	EM-AX0156
Chloroform	EMD Millipore	CX1058
Sucrose	Research Products International Corporation	S24060
Glutamine	Sigma	49419
Potassium phosphate dibasic	Sigma	P3786
Potassium Phosphate Monobasic	Sigma	P0662
Isopropanol	Honeywell	34965
Ammonium bicarbonate	Sigma	A6141
Phosphoric Acid	Sigma	49685
2:0 acyl-CoA	Avanti Polar Lipids	870702
4:0 acyl-CoA	Avanti Polar Lipids	870704
6:0 acyl-CoA	Avanti Polar Lipids	870706
8:0 acyl-CoA	Avanti Polar Lipids	870708
10:0 acyl-CoA	Avanti Polar Lipids	870710
12:0 acyl-CoA	Avanti Polar Lipids	870712
14:0 acyl-CoA	Avanti Polar Lipids	870714
16:0 acyl-CoA	Avanti Polar Lipids	870716
18:0 acyl-CoA	Avanti Polar Lipids	870718
16:1 acyl-CoA	Avanti Polar Lipids	870743
18:1 acyl-CoA	Avanti Polar Lipids	870731
Ammonium sulfate	Sigma	A4915
Flavin adenine dinucleotide (FAD)	Sigma	F8384
Bovine Serum Albumin (BSA)	Sigma	A7030
Triton X-100	Sigma	X100PC
Polyvinylpolypyrrolidone (PVP)	Sigma	PVP360
Protease inhibitor	Fisher Scientific	78430
Horseradish peroxidase	Sigma	P8250
p-hydroxybenzoic acid	Sigma	240141
4-amino antipyrine	Sigma	06800
Hydrogen peroxidase	Sigma	216763
Deposited data		
Mass Spectrometry Raw Data	Zenodo	Zenodo Data: https://doi.org/10.5281/zenodo.14393795

(*Continued on next page*)

Continued

REAGENT or RESOURCE	SOURCE	IDENTIFIER
Mass Spectrometry Raw Data	Zenodo	Zenodo Data: https://doi.org/10.5281/zenodo.14396946
Experimental models: Organisms/strains		
Camelina sativa: WT	Lab Stock	N/A
Brassica napus: WT	Lab Stock	N/A
Nicotiana tabacum: High-oil line	Commonwealth Scientific and Industrial Research Organisation (Australia)	N/A
Camelina sativa: High-oil lines	Lab Stock	FL3-1, CAT A7
Software and algorithms		
Origin Pro	OriginLab	https://www.originlab.com/
Plant Gramene database	Gramene	http://www.gramene.org
Thermo Xcalibur	Thermo Fisher Scientific	OPTON-30966
The Arabidopsis Information Resource database	Tair	https://www.arabidopsis.org/
Other		
DB23 column	Agilent Technologies	122-2332E
C8 column	Macherey-Nagel	Custom15M5
Acquity UPLC CSH C18 column	Waters	186005296

EXPERIMENTAL MODEL AND STUDY PARTICIPANT DETAILS

Plant materials and growth conditions

Camelina (*Camelina sativa* cv. Celine), rapeseed (*Brassica napus* cv. Reston), and tobacco (*Nicotiana tabacum* cv. Wisconsin 38) were used for this study. Transgenic high-oil tobacco lines were provided by the Commonwealth Scientific and Industrial Research Organisation (Australia).[38] Transgenic camelina lines were produced in the University of Missouri by our team.[4] All plants were grown at the Donald Danforth Plant Science Center. Greenhouses for camelina and rapeseed were maintained at 22°/20°C (day/night), approximately 50% relative humidity and a 16-h day (06:00 to 22:00 h) and an 8-h night (22:00 to 06:00 h) photoperiod. Natural light varied throughout the seasons; however, sunscreen cloths helped maintain a maximum of 500 μmol m^{-2} s^{-1} on bright summer days with a minimum light level of 250 μmol m^{-2} s^{-1} maintained by a combination of 600-W high-pressure sodium and 400-W metal halide bulbs. Tobacco plants were grown at a 14-h day cycle (08:00 to 22:00 h, 27°C) and 8-h night cycle (22:00 to 08:00 h, 25°C). On cloudy days, the light intensity was maintained at a minimum of 500 μmol m^{-2} s^{-1} using supplemental lighting.

METHOD DETAILS

Labeling studies

Isotope tracers were purchased from Sigma-Aldrich (St. Louis, MO, USA). Isotopic glucose (U-$^{13}C_6$) was fed to siliques containing mid-filling seeds for 4 and 8 h for ACP analysis and for 8 h for acyl-CoA analysis using the established silique culturing technique.[53] Additionally, intact seeds were supplemented with ^{18}O water ($H_2{}^{18}O$, 50%) for 30 min in a 50 mM sucrose and glutamine solution based on the imported metabolites in mid-filling camelina seeds.[53]

Sample collection

Photoperiod samples were collected every 4 h at 02:00, 06:00, 10:00, 14:00, 18:00, and 22:00 h. All other samples were collected at 10:00 h. For labeling experiments, siliques were harvested around 09.45 h and feeding experiments were initiated around 10:00 h. Samples were flash frozen in liquid nitrogen and stored at −80°C until further analysis.

Enzyme activity assay

Using a previous method,[32] protein for ACX activity was extracted from 100 mg (fresh weight) samples of early, mid, and late staged camelina seeds during seed filling, and 2-day old germinating seedlings. ACX enzyme activity was assessed by quantifying the H_2O_2 production rate at a wavelength of 500 nm[32] in a spectrophotometer (Plate reader Infinite 200 PRO, Tecan, Männedorf, Switzerland). 4:0, 8:0, 16:0, 18:1 and 18:3 acyl-CoAs were used individually as substrates for the enzyme activity assay. To account for potential contamination of CoAs and activity due to existing cellular acyl-CoA pools, blank samples included all components of the reaction mixture except the acyl-CoA substrate. To calculate final enzyme activity rates, the blank value was subtracted from the measured values.

Extraction of CoAs, ACPs and their measurements in LC-MS

Acyl-, enoyl-, dienoyl- and ketoacyl-CoAs were extracted following previous protocols[37,57] with modifications. The first extraction buffer consisted of chloroform and methanol (1:2 v/v) and was stored at −20°C until use. The second extraction buffer was freshly prepared by adding 50 mM KH_2PO_4, acetic acid and isopropanol (40:1:20 v/v). A mixture of 1 μM $^{13}C_3$ and 0.25 μM $^{13}C_{16}$ acyl-CoAs was used as internal standards in unlabeled samples to account for sample loss for quantification. Approximately 120 mg samples were used for one replicate but were divided into six sub-replicates to increase extraction efficiency. 500 μL of the first buffer and 2 μL of the internal standard mixture were added to each sub-replicate and stirred with beads using a bead beater for 2 min at −20°C. After adding 500 μL of the second buffer, another round of bead beating was performed at 4°C. 10 μL of saturated ammonium sulfate [$(NH_4)_2SO_4$] was added to the sample and shaken at 4°C for 2 h. After samples were centrifuged at 4°C and 20,000 g for 10 min, the upper phase of all six sub-replicates was pooled in a 15 mL tube for one replicate. Samples were dried in a SpeedVac concentrator and stored at −80°C.

Following a recent protocol[58] with modifications, CoAs were measured on a TSQ Altis triple quadrupole mass spectrometer (MS) connected to a Dionex UltiMate 3000 liquid chromatography (LC) system (Thermo Fisher Scientific, Waltham, MA, USA). In the LC, 10 mM ammonium bicarbonate in water was used as mobile phase A and 95% acetonitrile in water as mobile phase B. Analytes were separated using an Acquity UPLC CSH C18 column (1.7 μm × 2.1 mm × 50 mm). Samples were dissolved in 100 μL of solution containing mobile phase A and B and acetic acid (80:15:5 v/v) by sonication for 30 min at 4°C, centrifuged and filtered using 0.8μm PES membrane filters (Sartorius, Göttingen, Germany). Each LCMS run included three injections: one sample injection and two acid wash injections. To reduce carryover in LC column, 25 μL of an acid wash sample consisting of a mixture of phosphoric acid, water, and acetonitrile (5:40:60 v/v) was injected at mobile phase B proportions of 50% and 80% during the column equilibration phase, and the eluent was diverted to waste before entering the MS system. For ionization, the spray voltage was set at 4 kV in positive mode. The ion transfer tube and vaporizer temperature were set at 325°C and 350°C, respectively. The sheath, auxiliary and sweep gas flow rates were set to 45, 7 and 1 arbitrary units, respectively. The LC gradient and compound-dependent MS parameters for CoA are mentioned in Data S7.

Sample extraction and label measurement in acyl-ACPs were performed using previous methods.[25,43,52] ^{13}C-touched pool was calculated by summing all isotopologues (ΣM1-Mn isotopologues, where n is the number of carbon atoms) except the completely unlabeled isotopologue, i.e., M0.[52]

Lipid extraction and measurements in LC-MS

The amount of total lipid was measured by transesterification of fatty acids to fatty acid methyl esters (FAMEs) as previously detailed.[59] FAMEs were quantified by gas chromatography–flame ionization detection using a DB23 column (30 m, 0.25 mm i.d., 0.25 μm film: J&W Scientific, Folsom, USA) as described.[53]

Species of lipids were extracted using a variation of the previous protocol.[60] Homogenized sample material was extracted with a pre-chilled mix of methanol and methyl *tert*-butyl ether (1:3 v/v) that was spiked with UltimateSPLASH ONE mix (Avanti Polar Lipids, Alabaster, AL, USA) as internal standards. Samples were bead beaten for 30 s, incubated for 10 min in a shaker at 4°C, and then incubated for another 10 min in an ultra-sonication bath at room temperature. Phase separation was induced by adding 25% methanol in water to each sample tube. After centrifugation, the upper organic layer was aliquoted to a new tube and dried down in a SpeedVac concentrator. Samples were analyzed in LC-MS using a Q Exactive mass spectrometer coupled to a Dionex UltiMate 3000 UHPLC system (Thermo Fisher Scientific). A C8 column (5 μm × 150 mm x 0.5 mm) was used for chromatographic separations. Mobile phase A consisted of water with 1% 1 M ammonium acetate and 0.1% acetic acid, and mobile phase B consisted of 7:3 acetonitrile: isopropanol with 1% 1 M ammonium acetate and 0.1% acetic acid. The mass spectrometer acquired both positive and negative mode full scan mass spectra (MS1) from a single injection using polarity switching. For ionization, the spray voltage was set at 4 kV for positive mode and 3.9 kV for negative mode. The capillary and auxiliary gas heater temperature were set at 250°C and 60°C, respectively. The declustering potential (RF lens) was set to 50 V. The sheath and auxiliary gas flow rates were set to 15 and 5 arbitrary units, respectively. LC gradient data-dependent MS1 and MS2 parameters and quantitative method details of measured lipid species are mentioned in Data S8.

Bioinformatics

Proteins specific to lipase activity and straight-chain fatty acid breakdown were selected from Arabidopsis. Homologous proteins in camelina were identified using the Gramene database.[61] The extracted homologous proteins were annotated with gene symbols and descriptions based on the TAIR11 protein database[62] to ensure consistent and accurate functional characterization. The abundance and expression of identified camelina protein candidates were extracted from a previous study and reanalyzed for comparison between different developmental stages.[45]

QUANTIFICATION AND STATISTICAL ANALYSIS

Mass spectrometry-based metabolite quantification

Mass spectrometry-based CoA, ACP, and lipid data integration was performed within the Quant Browser software available from the Thermo Xcalibur Suite. Sample recoveries and extraction efficiency were calculated based on the internal standards which are

described in the Method Details section. Relative peak areas were calculated for individual lipid and CoA molecular species after normalization for the extraction efficiency and biomass used for extraction.

Statistical analysis

Two-tailed unequal variance Student's t tests were performed in Microsoft Excel to understand the significance in the difference in CoA abundances between different developing stages within each plant group and also between plant group (Figure 2, Data S2), difference in lipid abundance between three developmental stages of camelina seeds (Figure 3B and S4, Data S3), difference in transcript and proteomics abundances of fatty acid oxidation related genes between early-oil filling and germinating seedling stages (Figure 4B), and difference in oil content, ^{13}C incorporation rate, ratio of turnover and synthesis-specific ^{13}C acyl-CoA pool between wild-type and two engineered lines of camelina (Figures 6A–6C). A volcano plot was generated in the Origin Pro software to show the upregulated lipase genes with statistically significant fold-changes at the early oil-filling stage compared to germinating seedlings. To evaluate the cluster of CoA production during the photoperiod, principal component analysis (PCA) and k-means clustering analyses were performed (Figure 5). Data from at least three biological replicates are presented in all figures. The statistical test and data presentation (mean ± SD or SE) for each individual experiment is indicated in the figure legends. Statistical significance at $^{*}p < 0.05$, $^{**}p < 0.03$, and $^{**}p < 0.01$ is indicated in the figure legends.